



Published in final edited form as:

Appl Radiat Isot. 2014 September ; 91: 135–140. doi:10.1016/j.apradiso.2014.05.019.

Automated radiochemical synthesis and biodistribution of [¹¹C]- α -acetylmethadol ([¹¹C]LAAM)

Kiran Kumar Solingapuram Sai^{a,1}, Jinda Fan^{a,2}, Zhude Tu^a, Patrick Zerkel^a, Robert H. Mach^{a,3}, and Evan D. Kharasch^{b*}

^aDepartment of Radiology, Washington University in St. Louis, St. Louis, MO 63110 USA

^bDepartment of Anesthesiology, and Department of Biochemistry and Molecular Biophysics, Washington University in St. Louis, St. Louis, MO 63110 USA

Abstract

Long-acting opioid agonists methadone and *l*- α -acetylmethadol (LAAM) prevent withdrawal in opioid-dependent persons. Attempts to synthesize [¹¹C]-methadone for PET evaluation of brain disposition were unsuccessful. Owing, however, to structural and pharmacologic similarities, we aimed to develop [¹¹C]LAAM as a PET ligand to probe the brain exposure of long-lasting opioids in humans. This manuscript describes [¹¹C]LAAM synthesis and its biodistribution in mice. The radiochemical synthetic strategy afforded high radiochemical yield, purity and specific activity, thereby making the synthesis adaptable to automated modules.

Keywords

PET; *l*- α -acetylmethadol; LAAM; methadone; biodistribution; positron emission tomography

Introduction

Long-acting opioids are a mainstay in the treatment of pain and opioid addiction. Methadone (Figure 1), a long-duration mu opioid receptor agonist is used to treat acute, chronic, and cancer pain and has been in clinical use for decades.(Chou et al., 2009; Kharasch, 2011; Nicholson, 2007) Methadone is also used in maintenance therapy to treat opiate addiction and prevent opiate withdrawal.(Lobmaier et al., 2010) *levo*- α -acetylmethadol (LAAM,

© 2014 Published by Elsevier Ltd.

This manuscript version is made available under the CC BY-NC-ND 4.0 license.

* Address correspondence to: Evan D. Kharasch, M.D., Ph.D., Department of Anesthesiology, Washington University in St. Louis, 660 S. Euclid Ave., Campus Box 8054, St. Louis, Mo. 63110, Voice: (314) 362-8796, Fax: (314) 747-3371, kharasch@wustl.edu.

¹Present address: Department of Radiology, Wake Forest School of Medicine, 1 Medical Center Blvd, Winston Salem, NC 27157, USA

²Present address: Department of Radiology, University of Alabama School of Medicine, 720 2nd Ave S, Birmingham, AL 35294, USA

³Present address: Department of Radiology, Perelman School of Medicine, University of Pennsylvania, 231 S. 34th street, Philadelphia, PA 19104, USA

Publisher's Disclaimer: This is a PDF file of an unedited manuscript that has been accepted for publication. As a service to our customers we are providing this early version of the manuscript. The manuscript will undergo copyediting, typesetting, and review of the resulting proof before it is published in its final citable form. Please note that during the production process errors may be discovered which could affect the content, and all legal disclaimers that apply to the journal pertain.

levomethadyl acetate, (Figure 1) is another long-duration mu opioid receptor agonist, a structural analogue of methadone approved by the FDA in 1993 as an alternative to methadone for the prevention of opioid withdrawal and treatment of opiate addiction. (Kreek and Vocci, 2002; Tetrault and Fiellin, 2012) Clinical use of LAAM was low, for a variety of reasons, and the drug was withdrawn from clinical use in 2003.

Methadone disposition and clinical effects are susceptible to drug-drug interactions. For example antiretroviral drugs altered methadone plasma concentration-effect relationships (pharmacodynamics), suggesting altered methadone brain access, a potential role for drug transporters in human brain methadone disposition, and blood-brain barrier-mediated methadone-drug interactions. (Kharasch et al., 2008; Kharasch et al., 2009; Kharasch et al., 2012) Although these increased clinical effects suggested greater methadone brain concentrations, more direct evidence for increased brain concentrations was absent.

Positron emission tomography (PET) has emerged as a valuable approach for characterizing the brain pharmacokinetics of drugs in humans. (Matthews et al., 2012; Varnäs et al., 2013) More specifically, PET has been used extensively to understand the biology of opioid receptors and the pharmacology of opioids in humans. (Hammers and Lingford-Hughes, 2007; Henriksen and Willoch, 2008; Lever, 2007) Numerous radiolabelled opioids have been developed for PET imaging. (Dannals, 2013) Our initial objective was to develop a method for the synthesis of [^{11}C]methadone, to be used in human PET studies of methadone brain exposure. The synthesis and application to PET studies of [^{11}C]methadone had been described previously in abstract form. Ultimately, despite various synthetic approaches this proved unsuccessful. (YS Ding, 1996) Owing to the structural and pharmacologic similarity of methadone and LAAM, we therefore aimed to develop [^{11}C]LAAM as a PET ligand to probe the brain exposure of long-lasting opioids in humans. This manuscript describes the development and validation of [^{11}C]LAAM chemical synthesis, and [^{11}C]LAAM biodistribution studies in mice, using micro-PET.

Materials and Methods

All reagents and solvents were purchased from Sigma-Aldrich Chemical Co. (St. Louis, MO) except where noted. *l*- α -acetyl-*N*-normethadol HCl (norLAAM, the precursor used for C-11 labeling) and LAAM were provided by the National Institute of Drug Abuse (Rockville, MD) and supplied by Research Triangle Institute, NC. Radioactivity measurements were made in a Capintec CRC-712MV radioisotope dose calibrator (Capintec Inc., Ramsey, NJ). Water was purified by a Milli-Q integral water purification system (Millipore, Billerica, MA). Radiochemical yields (RCY) were calculated after the HPLC purification based on the total radioactivity trapped in the reaction vessel at the start of the reaction. Specific activities, decay corrected to end of synthesis (EOS) and recorded in mCi/ μmol , were determined from the carbon-11 activity in the product peak from the HPLC and the mass of compound (determined by the UV absorbance of the radioligand and the use of calibration curves of unlabeled reference compounds). Total synthesis times were calculated from end of bombardment (EOB) to end of radiotracer formulation.

Radiochemical synthesis of [¹¹C]LAAM

Production of [¹¹C]Methyl iodide (MeI)—[¹¹C]MeI was produced in the Washington University School of Medicine Cyclotron Facility with a Japan Steel Works BC-16/8 Cyclotron. A nitrogen target containing 0.2% oxygen was irradiated for 15–30 min with 40 μA beam of 16 MeV protons, to produce up to 1.4 Ci of [¹¹C]CO₂. The automated module, GE PET-trace FXM converts [¹¹C]CO₂ to [¹¹C]methane using a nickel catalyst [(Shimalite-Ni (reduced), Shimadzu, Japan P.N 221-27719)] at 360°C. [¹¹C]Methane was reacted with gaseous iodine at 720°C to form [¹¹C]MeI. (Larsen et al., 1997) The resultant [¹¹C]MeI gas was shunted through a NaOH column, to scavenge free iodide or HI (hydrogen iodide) and then passed through a PEEK column packed with silver triflate and heated to 200°C where it was converted to [¹¹C]methyl triflate ([¹¹C]MeOTf). (Tu et al., 2005) Approximately 12 minutes following the end-of-bombardment (EOB), several hundred millicuries of [¹¹C]MeOTf is delivered in the gas phase to the hot cell designated for the synthesis.

[¹¹C]LAAM synthetic procedure—A hot cell equipped with air-activated valves for remote manipulation for delivery and transfer of chemical solutions was used to carry out the radiosynthesis of [¹¹C]LAAM. The following accessories were used with the HPLC system in the hot cell: rheodyne injector valve with sample loop (2.0 mL), Thermo Separations HPLC binary pump (P200), Spectra-Physics UV variable wavelength detector, Bioscan flow counter radioactivity detector (NaI crystal), dual-pen chart recorder, and a three-way collection valve.

The radiosynthesis of [¹¹C]LAAM is represented in scheme 1. In a cone-shaped reaction vial, 0.6–0.7 mg of norLAAM is dissolved in 250 μL anhydrous methylethylketone (MEK) or 2-butanone, 4.0 μL of 30% potassium hydroxide (KOH) solution is added to this solution 4 minutes ahead of inlet of [¹¹C]MeOTf, which is then introduced to the reaction mixture by delivery with nitrogen carrying gas with a needle under the solution surface. The sealed reaction vial was heated at 60°C for 5 min. The reaction mixture was then quenched with 1.0 mL of HPLC mobile phase (48% acetonitrile: 52% 0.1 M ammonium formate pH 4.0–5.0 buffer) via the addition loop. The radioactive reaction mixture was then injected onto a reverse-phase Agilent Zorbax C18 semi-preparative HPLC column (250 × 9.6 mm, 5 μ) for purification. The HPLC mobile phase solution was 48% acetonitrile, 52% 0.1 M aqueous ammonium formate buffer (pH 4.5), with UV wavelength at 225 nm, at a flow rate of 3.5 mL/min. Under these conditions, [¹¹C]LAAM was collected between 14.0–16.5 min in a vial of sterile water (50 mL). A typical HPLC trace is represented in Figure 2. The radioactive solution was then passed through a C18 SepPak cartridge (WAT020515, Waters Corp, Milford, MA), where the [¹¹C]LAAM was trapped. The radioactive product was eluted with absolute ethanol (1.0 mL) and concentrated under reduced pressure then formulated with 10% absolute ethanol in saline. The final dose was filtered using a sterile 0.22 μm pyrogen-free Millipore filter (Millipore Corp., Billerica, MA) into the dose vial for animal studies and quality control analysis.

Quality control analysis of [¹¹C]LAAM—Quality control testing of [¹¹C]LAAM was conducted using guidelines in the US pharmacopeia by standard tests as described earlier (Fan et al., 2011) and the specific release criteria are reported in Table 1.

The chemical and radiochemical purity of the collected radioactive aliquot was checked by performing a HPLC injection on an Agilent C18 analytical column (250×4.6 mm, 5 μm). The mobile phase was 45% acetonitrile and 55% 50 mM aqueous ammonium phosphate buffer (pH 2.7); the UV detection was set at 225 nm with a flow rate of 1.5 mL/min. Under these QC HPLC conditions, the single injection of [¹¹C]LAAM had a retention time of 5.28 min as represented in Figure 3. The radioactive peak was further authenticated by performing a co-injection with nonradioactive standard LAAM, which displayed a similar retention time.

Biodistribution studies

All animal experiments were conducted in compliance with the Guidelines for the Care and Use of Research Animals established by Washington University's Animal Studies Committee. For the biodistribution studies, 100–130 μCi of [¹¹C]LAAM in 100–120 μL of saline containing 10% ethanol was injected via the tail vein into normal Swiss-Webster male mice (25–50 g) under 2–3% isoflurane/oxygen anesthesia. Group of mice (n = 4) were used for each time point. At 5, 15, 30, 60 and 90 min post i.v. injection, the mice were anesthetized and euthanized. At these time points, samples of blood, lungs, liver, spleen, kidneys, bladder, muscle, fat, heart, brain, bone, marrow, testes, prostate, adrenals, thyroid, pancreas, stomach, small intestines, upper and lower large intestines. The 90 min group of animals was maintained in metabolic cages where urine and feces excretion were collected, weighted and counted for radioactivity in a Beckman Gamma 8000 well counter with a standard dilution of the injectate. Tissues were weighed, and the %I.D./g for each tissue was calculated.

Results and Discussion

[¹¹C]LAAM Radiochemistry

The C-11 alkylation of nor-LAAM was investigated using different reaction conditions (Table 2). Alkylation was initially carried out with [¹¹C]MeI and then later shifted to stronger [¹¹C]MeOTf to facilitate alkylation towards *N*-methylation. For optimal radiochemical yields the reaction was heated to 60°C, even though usage of stronger methylating agent like MeOTf often does not require temperatures higher than 20–25°C. One explanation could be the sterically hindered structure of the nor-LAAM precursor; however, the exact cause is not evident. Several bases including 5N sodium hydroxide (NaOH) aqueous solution, 1M cesium carbonate (Cs₂CO₃) aqueous solution, and 30% KOH aqueous solution were used as bases during the radiochemical synthesis; however, 30% KOH aqueous solution yielded [¹¹C]LAAM in higher radiochemical yields (RCY) and purity. Among MEK and dimethylsulfoxide (DMSO), MEK was chosen as the suitable reaction solvent due to its aprotic behavior and high radioactivity trapping nature, especially with [¹¹C]MeOTf. (Iwata et al., 2001; Nagren et al., 1995) The reaction temperature of 60°C was found to be suitable for the alkylation with [¹¹C]MeOTf, as higher temperatures tend to

form some undesirable radioactive side products, lowering RCY. [^{11}C]MeOTf, MEK, 30% KOH and 60°C were found to be the ideal methylating agent, solvent, base and temperature respectively for the synthesis of [^{11}C]LAAM.

The total time required for the synthesis of [^{11}C]LAAM, including [^{11}C]MeOTf production, purification and formulation was approximately 50 min. The radiochemical purity of [^{11}C]LAAM was >99% and was confirmed by co-elution with non-radioactive LAAM. The chemical purity of [^{11}C]LAAM determined by the HPLC UV mass was >99%. The calculated radiochemical yield was ~55–63% (n=12) after the HPLC purification and the final product had a specific activity of 3,000–5,200 mCi/ μmol (n=12), decay-corrected to end of synthesis. The final [^{11}C]LAAM dose met all the established release criteria as summarized in Table 1, thus confirming its clinical suitability in PET imaging studies.

Biodistribution studies

The radioactivity distribution of [^{11}C]LAAM in normal Swiss-Webster male mice organs is summarized in Table 3. For [^{11}C]LAAM biodistribution, lung had the highest amount of radioactive uptake among the tissues that were analyzed. Uptake (%I.D./g) in lung reached 67.8 ± 7.3 at 5 min, 30.1 ± 2.8 at 30 min and 12.9 ± 2.6 at 90 min, and a 5-fold decrease in radioactivity was observed from 5 min to 90 min. The uptake in blood was low; 1.11 ± 0.16 (%I.D./g) in 5 min and it remained uniform even after 90 min. Brain uptake was 1.91 ± 0.32 and 1.52 ± 0.13 at 15 and 30 min. This was slightly less than or comparable to brain uptake of the structurally unrelated anilidopiperidine opioid [^{11}C]carfentanil. (Jewett and Kilbourn, 2004)

Comparative synthesis of [^{11}C] long-acting opioids

Methadone is the primary long-acting opioid of clinical and research interest, and initial efforts were directed at the synthesis of [^{11}C]methadone. Several efforts were made to synthesize [^{11}C]methadone; including [^{11}C]methylation after *N*-demethylation of methadone, and *de novo* synthesis and remethylation, however, none were successful. Direct methylation of *N*-desmethylmethadone failed under several reaction conditions, including varying reaction temperature, time, solvent and base due to the chemically unstable nature of *N*-desmethylmethadone, which is well known to rearrange and cyclize spontaneously to 2-ethylene-1,5-dimethyl-3,3-diphenylpyrrolidine. (YS Ding, 1996) Attempts to initial *N*-demethylation of the methadone followed by C11 remethylation via [^{11}C]MeI or [^{11}C]MeOTf yielded very less or no desired radiotracer.

In contrast to the synthesis of [^{11}C]methadone, the synthesis of [^{11}C]LAAM was easily attained and optimized for PET studies. The fundamental difference between the synthesis of the two [^{11}C]-methylated compounds was the stability of *l*- α -acetyl-*N*-normethadol. HCl (i.e., norLAAM, and its availability as a starting compound) compared with the instability of *N*-desmethylmethadone.

Conclusion

An automated chemical synthesis of [^{11}C]LAAM was successfully developed and performed on a GE-FXM module and the method was validated and approved for routine

clinical production for investigational studies. The radiochemical synthetic strategy afforded high radiochemical yield, purity and specific activity which would make the synthesis easy to perform and more adaptable to any other automated modules. Initial biodistribution studies in normal Swiss-Webster mice demonstrate high radioactive uptake in target organs and optimal clearance from kidney, pancreas and liver.

Acknowledgments

Funding sources: Supported by National Institute of Health grants R01DA14211, R01DA25931 and K24DA00417

References

- Chou R, Fanciullo GJ, Fine PG, Adler JA, Ballantyne JC, Davies P, Donovan MI, Fishbain DA, Foley KM, Fudin J, Gilson AM, Kelter A, Mauskop A, O'Connor PG, Passik SD, Pasternak GW, Portenoy RK, Rich BA, Roberts RG, Todd KH, Miaskowski C. Clinical Guidelines for the Use of Chronic Opioid Therapy in Chronic Noncancer Pain. *The Journal of Pain*. 2009; 10:113–130. [PubMed: 19187889]
- Dannals RF. Positron emission tomography radioligands for the opioid system. *Journal of Labelled Compounds and Radiopharmaceuticals*. 2013; 56:187–195. [PubMed: 24285325]
- Fan J, Meissner K, Gaele GG, Li S, Kharasch ED, Mach RH, Tu Z. Automated radiosynthesis of [¹¹C]morphine for clinical investigation. *Applied Radiation and Isotopes*. 2011; 69:431–435. [PubMed: 21112214]
- Hammers A, Lingford-Hughes A. Opioid Imaging. *PET Clinics*. 2007; 2:67–89.
- Henriksen G, Willoch F. Imaging of opioid receptors in the central nervous system. *Brain*. 2008; 131:1171–1196. [PubMed: 18048446]
- Iwata R, Pascali C, Bogno A, Miyake Y, Yanai K, Ido T. A simple loop method for the automated preparation of [¹¹C]raclopride from [¹¹C]methyl triflate. *Applied Radiation and Isotopes*. 2001; 55:17–22. [PubMed: 11339532]
- Jewett DM, Kilbourn MR. In vivo evaluation of new carfentanil-based radioligands for the mu opiate receptor. *Nucl Med Biol*. 2004; 31:321–325. [PubMed: 15028244]
- Kharasch ED. Intraoperative Methadone: Rediscovery, Reappraisal, and Reinvigoration? *Anesthesia & Analgesia*. 2011; 112:13–16. [PubMed: 21173206]
- Kharasch ED, Bedynek PS, Park S, Whittington D, Walker A, Hoffer C. Mechanism of Ritonavir Changes in Methadone Pharmacokinetics and Pharmacodynamics: I. Evidence Against CYP3A Mediation of Methadone Clearance. *Clin Pharmacol Ther*. 2008; 84:497–505. [PubMed: 19238655]
- Kharasch ED, Walker A, Whittington D, Hoffer C, Bedynek PS. Methadone metabolism and clearance are induced by nelfinavir despite inhibition of cytochrome P4503A (CYP3A) activity. *Drug and Alcohol Dependence*. 2009; 101:158–168. [PubMed: 19232844]
- Kharasch ED, Whittington D, Ensign D, Hoffer C, Bedynek PS, Campbell S, Stubbert K, Crafford A, London A, Kim T. Mechanism of Efavirenz Influence on Methadone Pharmacokinetics and Pharmacodynamics. *Clin Pharmacol Ther*. 2012; 91:673–684. [PubMed: 22398970]
- Kreek MJ, Vocci FJ. History and current status of opioid maintenance treatments: blending conference session. *Journal of Substance Abuse Treatment*. 2002; 23:93–105. [PubMed: 12220607]
- Larsen P, Ulin J, Dahlstrøm K, Jensen M. Synthesis of [¹¹C]iodomethane by iodination of [¹¹C]methane. *Applied Radiation and Isotopes*. 1997; 48:153–157.
- Lever JR. PET and SPECT Imaging of the Opioid System: Receptors, Radioligands and Avenues for Drug Discovery and Development. *Current Pharmaceutical Design*. 2007; 13:33–49. [PubMed: 17266587]
- Lobmaier P, Gossop M, Waal H, Bramness J. The pharmacological treatment of opioid addiction—a clinical perspective. *Eur J Clin Pharmacol*. 2010; 66:537–545. [PubMed: 20169438]
- Matthews PM, Rabiner EA, Passchier J, Gunn RN. Positron emission tomography molecular imaging for drug development. *British Journal of Clinical Pharmacology*. 2012; 73:175–186. [PubMed: 21838787]

- Nagren K, Halldin C, Muller L, Swahn CG, Lehtikoinen P. Comparison of [^{11}C]methyl triflate and [^{11}C]methyl iodide in the synthesis of PET radioligands such as [^{11}C]β-CIT and [^{11}C]β-CFT. *Nuclear Medicine and Biology*. 1995; 22:965–970. [PubMed: 8998473]
- Nicholson AB. Methadone for cancer pain. *The Cochrane database of systematic reviews*, CD003971. 2007
- Tetrault J, Fiellin D. Current and Potential Pharmacological Treatment Options for Maintenance Therapy in Opioid-Dependent Individuals. *Drugs*. 2012; 72:217–228. [PubMed: 22235870]
- Tu Z, Dence CS, Ponde DE, Jones L, Wheeler KT, Welch MJ, Mach RH. Carbon-11 labeled σ_2 receptor ligands for imaging breast cancer. *Nuclear Medicine and Biology*. 2005; 32:423–430. [PubMed: 15982571]
- Varnäs K, Varrone A, Farde L. Modeling of PET data in CNS drug discovery and development. *J Pharmacokinet Pharmacodyn*. 2013; 40:267–279. [PubMed: 23660778]
- Ding, YS.; JF; Volkow, ND.; Studebaker, R.; Pipolo, F. Synthesis and positron emission tomographic (PET) baboon studies of [^{11}C]methadone and R-(–)-[^{11}C]methadone *Journal of Nuclear Medicine Abstract, Journal Issue: Suppl.5; Conference: 43. Annual meeting of the Society of Nuclear Medicine; Denver, CO (United States)*. 1996. p. 40

Highlights

- Radiochemical synthesis of opioid [^{11}C]- α -acetylmethadol (LAAM) described for the first time
- High radiochemical yield, purity and specific activity
- Easily reproducible and adaptable synthesis to any C-11 automated modules
- [^{11}C]LAAM utility as a PET radiopharmaceutical for assessing brain penetration

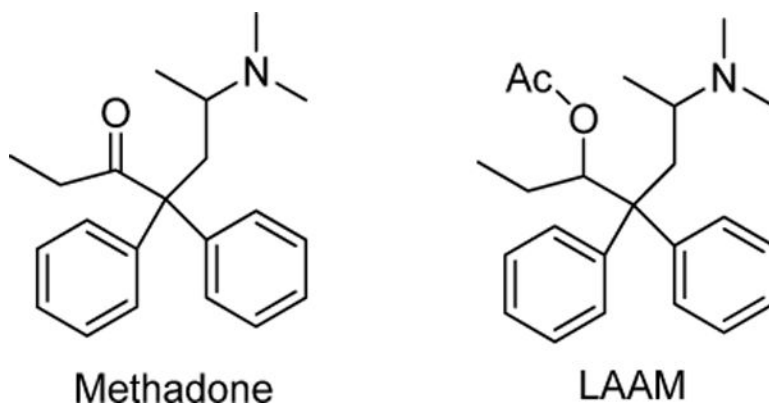


Figure 1.
Structures of methadone and *l*- α -acetylmethadol (LAAM).

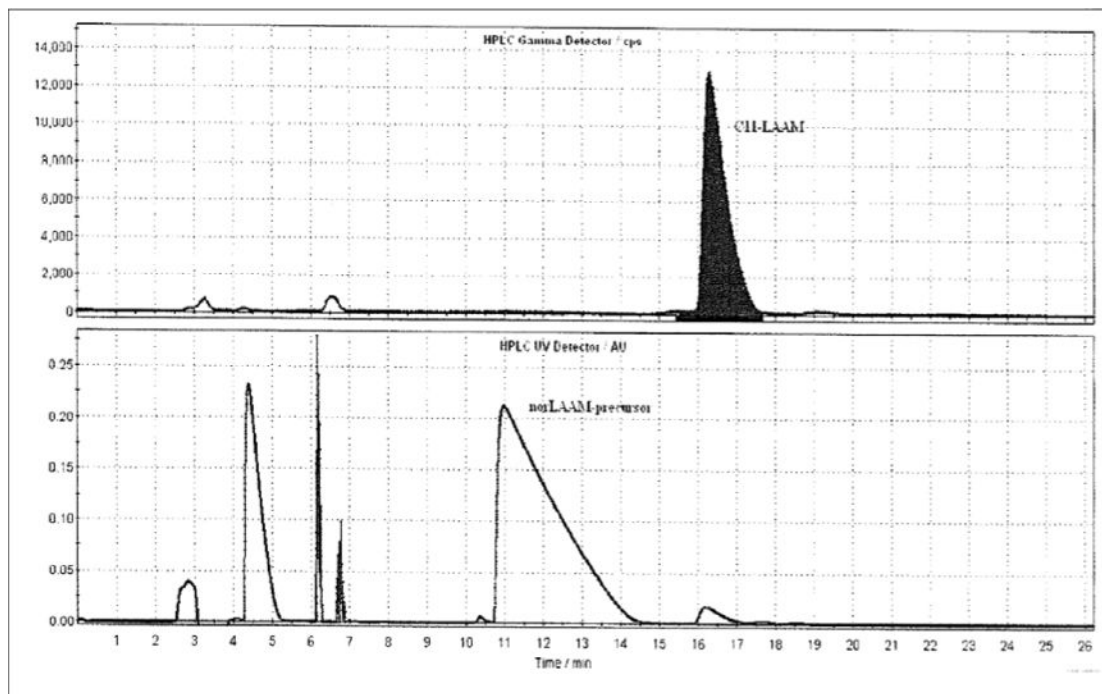


Figure 2.
Typical semipreparative HPLC of [^{11}C]LAAM: top window radioactivity in counts per second (CPS) and lower window UV in absorbance units (AU)

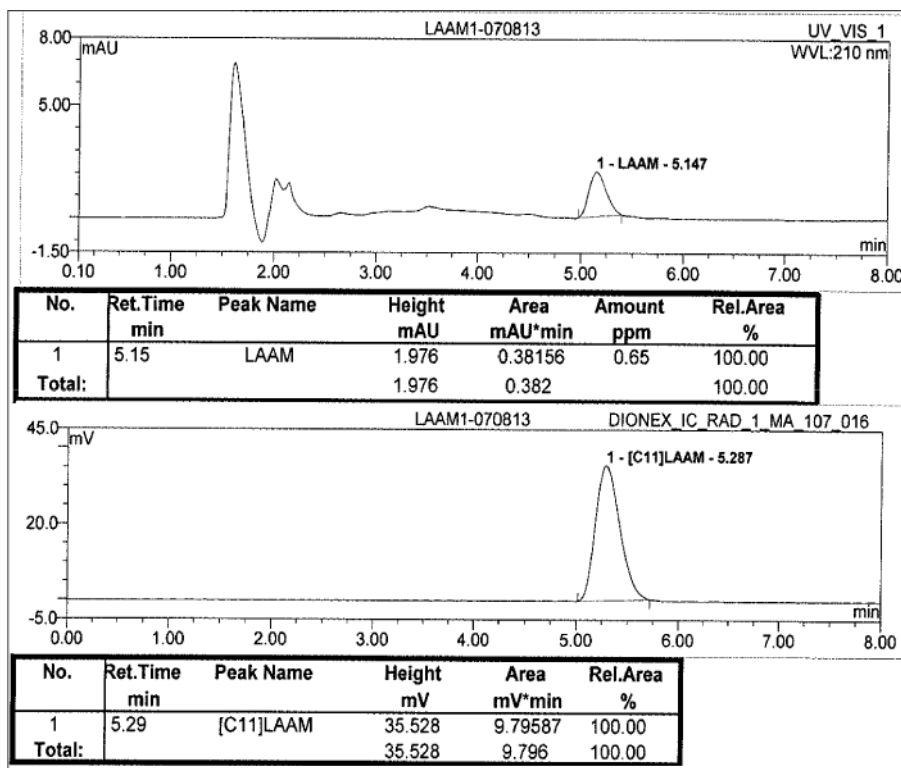
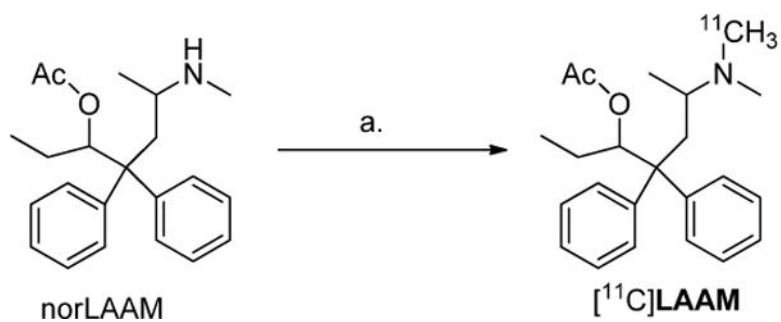


Figure 3. Typical analytical HPLC of [^{11}C]LAAM; top window UV in milli Absorbance Units (mAU) and bottom window radioactivity in milli volts (mV)

**Scheme 1.**

Reagents and conditions: (a) [^{11}C]MeOTf, 30% KOH, MEK, 60°C, 5 min.

Table 1Quality control release criteria for [¹¹C]LAAM

TEST	RELEASE CRITERIA
filter membrane integrity test	Should not rupture until 45 psi
visual appearance	Clear and particle-free; colorless
pH	4.5 – 8.0
strength	5.4–6.5Ci/mL
radionuclidic identity	19.37 to 21.40 minutes
radiochemical purity	90%
radiochemical identity	Radioactive peak and standard (or co-injection) mass peak retention times must agree by $\pm 10\%$
chemical purity; LAAM mass	10 μg
specific activity @ EOS	2000 mCi/ μmol
bacterial endotoxin	175 EU/V (where V is the maximum dose administered)
residual solvent: acetonitrile	0.41 mg/mL (4.1 mg/day max)
residual solvent: MEK	5.0 mg/mL (50 mg/day max)
ethanol	30–100 mg/mL
sterility	No visible growth
radionuclidic purity	99.5%

Table 2Reaction conditions and radiochemical yields for [¹¹C]LAAM

Solvent	Methylation source / base / reaction temperature	Radiochemical yield
DMSO	[¹¹ C]MeI / 5N NaOH/ 85°C	41%
DMSO	[¹¹ C]MeI / 1M Cs ₂ CO ₃ / 85°C	25%
DMSO	[¹¹ C]MeOTf / 5N NaOH/ 60°C	52%
MEK	[¹¹ C]MeOTf / 5N NaOH/ 60°C	58%
MEK	[¹¹ C]MeOTf / 30% KOH/ 60°C	63%

Author Manuscript

Author Manuscript

Author Manuscript

Author Manuscript

Table 3

Biodistribution of [¹⁴C]LAAM in male Swiss-Webster mice*.

Organ	5 min	15 min	30 min	60 min	90 min
blood	1.11 ± 0.16	1.05 ± 0.09	0.93 ± 0.10	1.10 ± 0.10	1.19 ± 0.11
lung	67.75 ± 7.28	53.16 ± 10.42	30.07 ± 2.77	19.12 ± 1.84	12.94 ± 2.61
liver	8.43 ± 0.96	8.92 ± 1.29	9.73 ± 1.76	8.55 ± 1.31	7.38 ± 1.07
spleen	6.43 ± 1.06	9.72 ± 2.08	8.88 ± 0.57	5.75 ± 0.69	4.49 ± 0.69
kidney	21.30 ± 1.26	16.58 ± 2.82	12.41 ± 1.69	6.78 ± 0.52	4.59 ± 0.60
bladder	1.92 ± 0.90	3.23 ± 0.72	6.38 ± 3.84	3.20 ± 1.32	3.57 ± 1.35
gall bladder	2.68 ± 0.47	3.62 ± 1.13	7.28 ± 3.03	13.16 ± 6.77	22.18 ± 5.72
muscle	4.22 ± 0.37	3.07 ± 0.65	1.96 ± 0.24	1.41 ± 0.12	1.01 ± 0.21
fat	2.32 ± 1.35	2.33 ± 0.58	3.72 ± 0.52	3.62 ± 0.74	4.79 ± 1.64
Heart	7.56 ± 1.14	4.56 ± 0.93	3.11 ± 0.75	1.85 ± 0.40	1.58 ± 0.60
brain	1.81 ± 0.14	1.91 ± 0.32	1.52 ± 0.13	1.07 ± 0.09	0.94 ± 0.15
bone	2.76 ± 0.43	3.51 ± 0.65	3.18 ± 0.42	2.01 ± 0.38	2.43 ± 1.05
marrow	2.91 ± 1.33	1.93 ± 1.19	2.07 ± 1.50	3.79 ± 3.17	3.26 ± 7.09
testes	1.32 ± 0.08	1.80 ± 0.35	2.06 ± 0.14	2.60 ± 0.43	2.42 ± 0.66
prostate	2.12 ± 0.77	2.82 ± 0.48	3.27 ± 1.65	2.17 ± 1.17	2.63 ± 0.97
adrenals	14.35 ± 0.59	8.68 ± 3.54	8.80 ± 1.82	4.78 ± 0.94	4.01 ± 3.66
thyroid	4.90 ± 0.31	3.97 ± 0.33	3.46 ± 0.58	2.26 ± 0.40	3.01 ± 1.82
pancreas	9.84 ± 1.69	8.13 ± 2.14	7.35 ± 1.03	5.44 ± 0.55	4.94 ± 0.69
thymus	4.93 ± 0.97	5.15 ± 1.33	4.88 ± 0.68	3.65 ± 0.65	2.16 ± 0.94
stomach	3.21 ± 0.68	3.68 ± 1.06	4.58 ± 0.38	3.36 ± 0.94	3.29 ± 0.74
small intestine	5.74 ± 0.41	6.76 ± 0.72	7.97 ± 0.85	7.05 ± 1.25	5.89 ± 0.89
upper large intestine	3.61 ± 0.17	4.53 ± 0.62	4.49 ± 0.37	6.13 ± 0.95	8.26 ± 1.66
lower large intestine	2.19 ± 0.14	2.30 ± 0.56	2.56 ± 0.08	2.22 ± 0.18	2.16 ± 0.35
skin	1.50 ± 0.10	2.02 ± 0.37	2.26 ± 0.21	2.35 ± 0.39	2.00 ± 0.49

* results are expressed as percent injected dose per gram of tissue (%ID/g) and are the mean ± standard deviation (n=4).